



On the Concept of Depth for Functional Data

Sara López-Pintado & Juan Romo

To cite this article: Sara López-Pintado & Juan Romo (2009) On the Concept of Depth for Functional Data, *Journal of the American Statistical Association*, 104:486, 718-734, DOI: [10.1198/jasa.2009.0108](https://doi.org/10.1198/jasa.2009.0108)

To link to this article: <https://doi.org/10.1198/jasa.2009.0108>



Published online: 01 Jan 2012.



Submit your article to this journal 



Article views: 1413



View related articles 



Citing articles: 69 View citing articles 

On the Concept of Depth for Functional Data

Sara LÓPEZ-PINTADO and Juan ROMO

The statistical analysis of functional data is a growing need in many research areas. In particular, a robust methodology is important to study curves, which are the output of many experiments in applied statistics. As a starting point for this robust analysis, we propose, analyze, and apply a new definition of depth for functional observations based on the graphic representation of the curves. Given a collection of functions, it establishes the “centrality” of an observation and provides a natural center-outward ordering of the sample curves. Robust statistics, such as the median function or a trimmed mean function, can be defined from this depth definition. Its finite-dimensional version provides a new depth for multivariate data that is computationally feasible and useful for studying high-dimensional observations. Thus, this new depth is also suitable for complex observations such as microarray data, images, and those arising in some recent marketing and financial studies. Natural properties of these new concepts are established and the uniform consistency of the sample depth is proved. Simulation results show that the corresponding depth based trimmed mean presents better performance than other possible location estimators proposed in the literature for some contaminated models. Data depth can be also used to screen for outliers. The ability of the new notions of depth to detect “shape” outliers is presented. Several real datasets are considered to illustrate this new concept of depth, including applications to microarray observations, weather data, and growth curves. Finally, through this depth, we generalize to functions the Wilcoxon rank sum test. It allows testing whether two groups of curves come from the same population. This functional rank test when applied to children growth curves shows different growth patterns for boys and girls.

KEY WORDS: Data depth; Functional data; Rank test for functions.

1. INTRODUCTION

The data output sophistication in emerging research fields requires advancing the statistical analysis of complex data. In functional data analysis, each observation is a real function $x_i(t)$, $i = 1, \dots, n$, $t \in I$, where I is an interval in \mathbb{R} . There are several motivations for studying functional data. In many research areas (medicine, biology, economics, engineering), the data generating process is naturally a stochastic function. Moreover, many problems are better approached if the data are considered as functions. For instance, if each curve is observed at different points, a multivariate analysis would not be valid, and it is therefore necessary to smooth the data and treat them as continuous functions defined in a common interval. Even if the data are observed at the same time points, a standard multivariate analysis might not be computationally feasible due to the curse of dimensionality because the dimension is often significantly higher than the number of curves observed.

Multivariate techniques, such as principal components, analysis of variance, and regression methods, have already been extended to a functional context (see Ramsay and Silverman, 2005). A fundamental task in functional data analysis is to provide an ordering within a sample of curves that allows the definition of order statistics, such as ranks and L -statistics. A natural tool to analyze these functional data aspects is the idea of statistical depth. It has been introduced to measure the “centrality” or the “outlyingness” of an observation with respect to a given dataset or a population distribution. In this article, we propose a new definition of depth for functional observations. It allows ordering a sample of curves from the center-outward and, thus, extending robust statistics to a func-

tional context. For example, a median function is a curve with the highest depth.

The notion of depth was first considered for multivariate data to generalize order statistics, ranks, and medians to higher dimensions. Given a distribution of probability F in \mathbb{R}^d , a statistical depth assigns to each point \mathbf{x} a real nonnegative bounded value $D(\mathbf{x}, F)$. Several depth definitions for multivariate data have been proposed and analyzed by Mahalanobis (1936), Tukey (1975), Oja (1983), Liu (1990), Singh (1991), Fraiman and Meloche 1999, Vardi and Zhang (2000), Koshelovoy and Mosler (1997) and Zuo (2003), among others. Liu (1990) and Zuo and Serfling (2000a) introduced and studied key properties a depth should satisfy. Dyckerhoff (2004) also considered desirable properties for multivariate depths. Data depth can be widely applied. For example, Liu and Singh (1993) presented a nonparametric multivariate rank test using a quality depth index and Liu (1995) proposed control charts for multivariate processes using depth. Yeh and Singh (1997) studied confidence sets based on Tukey’s depth. Also, Liu, Parelius, and Singh (1999) offered depth tools for multivariate analysis; for instance, they defined trimmed regions, central regions and contours, and constructed a scale curve to visualize sample dispersion. Mosler (2002) analyzed central regions and multivariate dispersions based on the lift zonoid approach. In addition, Rousseeuw and Hubert (1999) introduced the idea of regression depth and Li and Liu (2004) designed a graphic tool and a test to check if two multivariate samples come from the same population. Direct generalization of current multivariate depths to functional data often leads to either depths that are computationally intractable or depths that do not take into account some natural properties of the functions, such as shape. Vardi and Zhang (2000) proposed the L_1 -depth for multivariate data, which is computationally feasible in high dimensions and therefore can be extended to functional data. This depth was also analyzed by Serfling (2004) in the context of spatial rank functions, and it is also closely related and motivated by the geometric quantiles for multivariate data introduced in

Sara López-Pintado is Assistant Professor, Department of Economics, Quantitative Methods and Economic History, Universidad Pablo de Olavide, Sevilla, Spain (E-mail: sloppin@upo.es). Juan Romo is Professor, Department of Statistics, Universidad Carlos III de Madrid, Getafe, Madrid, Spain (E-mail: juan.romo@uc3m.es). This research was supported in part by Spanish Ministry of Education and Science grants BEC2002-03769, SEJ2005-06454, SEJ2007-67734, and SEJ2905. The authors thank the editors and two referees for their helpful comments and suggestions. The authors also thank Juan Lin for his generous reading and comments on the manuscript and Francisco Rodríguez for the Laricio trees data set.

Chaudhuri (1996), who indicated, following the results in Kemperman (1987), that the geometric quantiles, in particular the median, could be extended to Hilbert and Banach spaces. Fraiman and Muniz (2001) defined and studied a concept of depth for functional observations based on the integrals of univariate depths. Recently, Cuevas, Febrero, and Fraiman (2007) have proposed a projection-based depth for functions.

The main goal of this article is to propose a new notion of depth for functional data. It is based on the graphic representation of the functions and makes use of the bands defined by their graphs on the plane. Its finite-dimensional version is an alternative definition of depth for multivariate data, satisfying properties studied in Zuo and Serfling (2000a), except affine invariance. In addition, it has the advantage of being computationally feasible, which is essential for analyzing high-dimensional data. Thus, this depth is the starting point for a new robust statistical methodology to study complex and high-dimensional observations as images or microarrays. Some asymptotic results, such as the uniform convergence of the sample depth and deepest point are established. Most of these properties are extended to functions. With this new definition we can also generalize the concepts of multivariate L -estimates (in particular, trimmed means) to a functional context. Robust methods are even more relevant in a functional setting than in multivariate problems because outliers can affect functional statistics in more ways, and they can be more difficult to detect. For instance, a curve could be an “outlier” without having any unusually large value. The depth we propose is particularly convenient for identifying this kind of outlier because in this case shape is also relevant in addition to magnitude.

The article is organized as follows. In Section 2, we present the new definition of band depth for functional data. Section 3 explores its finite-dimensional version and its properties. In Section 4, the functional depth properties are analyzed. A modified band depth, more convenient for irregular functions, is defined and studied in Section 5. Section 6 contains some simulations illustrating the robustness of estimates based on the proposed depth. Also, a comparison of the performance for detecting outliers of these new notions of depth and others proposed in the literature is presented. In Section 7, real data examples are discussed, showing the band depth performance. A microarray data example is included to illustrate the broad applicability of the new statistical depths. A rank test for functions is introduced in Section 8 and applied to the problem of deciding whether two groups of real curves come from the same population. Finally, in Section 9 we summarize the main conclusions of this article.

2. A BAND DEPTH FOR FUNCTIONAL DATA

Our proposal follows a graph-based approach. We recall definitions about function graphs that will be used throughout the article. Let $x_1(t), \dots, x_n(t)$ be a collection of real functions. Although the following ideas can be introduced for more general functional observations, we will restrict the exposition to functions in the space $C(I)$ of real continuous functions on the compact interval I . The graph of a function x is the subset of the plane $G(x) = \{(t, x(t)): t \in I\}$. The band in \mathbb{R}^2 delimited by the curves x_{i_1}, \dots, x_{i_k} is

$$\begin{aligned} B(x_{i_1}, x_{i_2}, \dots, x_{i_k}) &= \{(t, y) : t \in I, \min_{r=1, \dots, k} x_{i_r}(t) \leq y \leq \\ &\quad \max_{r=1, \dots, k} x_{i_r}(t)\} = \{(t, y) : t \in I, y = \alpha \\ &\quad \min_{r=1, \dots, k} x_{i_r}(t) + (1 - \alpha) \max_{r=1, \dots, k} x_{i_r}(t), \\ &\quad \alpha \in [0, 1]\}. \end{aligned}$$

Figure 1(a) presents the band $B(x_1, x_2)$ given by two curves; the graph of y_1 is included in the band, whereas the graph of y_2 is not completely inside the band. Figure 1(b) shows the band $B(x_1, x_2, x_3)$ defined by three curves. For any function x in x_1, \dots, x_n , and fixed j value with $2 \leq j \leq n$, the quantity

$$BD_n^{(j)}(x) = \binom{n}{j}^{-1} \sum_{1 \leq i_1 < i_2 < \dots < i_j \leq n} I\{G(x) \subseteq B(x_{i_1}, x_{i_2}, \dots, x_{i_j})\},$$

expresses the proportion of bands $B(x_{i_1}, x_{i_2}, \dots, x_{i_j})$ determined by j different curves $x_{i_1}, x_{i_2}, \dots, x_{i_j}$ containing the whole graph of x . ($I\{A\}$ is one if A is true and zero, otherwise).

Definition 1. Let J be a fixed value with $2 \leq J \leq n$. For functions x_1, \dots, x_n , the *band depth* of any of these curves x is

$$BD_{n,J}(x) = \sum_{j=2}^J BD_n^{(j)}(x). \quad (1)$$

If X_1, X_2, \dots, X_J are independent copies of the stochastic process X generating the observations x_1, \dots, x_n , the corresponding population versions are $BD^{(j)}(x, P) = P\{G(x) \subseteq B(X_1, X_2, \dots, X_j)\}$ and

$$BD_J(x, P) = \sum_{j=2}^J BD^{(j)}(x, P) = \sum_{j=2}^J P\{G(x) \subseteq B(X_1, X_2, \dots, X_j)\}.$$

We recommend considering the definition of band depth with $J = 3$ for several reasons: (1) when J is larger than 3 the index $BD_{n,J}$ can be computationally intensive, (2) bands corresponding to large values of J do not resemble the shape of any of the curves from the sample, (3) the band depth induced order is very stable in J , and (4) the band depth with $J = 2$ is the easiest to compute, but if two curves cross over, the band delimited by them is degenerated in a point and, with probability one, no other curve will be inside this band. Throughout the article we have considered the band depth with $J = 3$, although the theoretical properties can be proven for general J . For simplicity, we write $BD_3 = BD$ and $BD_{n,3} = BD_n$.

A sample median function \hat{m}_n is a curve from the sample with highest depth value, $\hat{m}_n = \arg \max_{x \in \{x_1, \dots, x_n\}} BD_n(x)$, and a pop-

ulation median is a function m in $C(I)$ maximizing $BD(\cdot)$. If they are not unique, the median will be the average of the curves maximizing depth.

The functions in Figure 2 represent the angle in the sagittal plane formed by the hip (left panel) and by the knee (right panel) as 39 children go through a gait cycle (see Ramsay and Silverman, 2005). The deepest curves (or median functions) for BD_n appear in red. The notion of functional depth allows ordering data curves from the center-outward and order based statistics can be defined; this provides a basis for generalizing L -statistics to the functional setting.

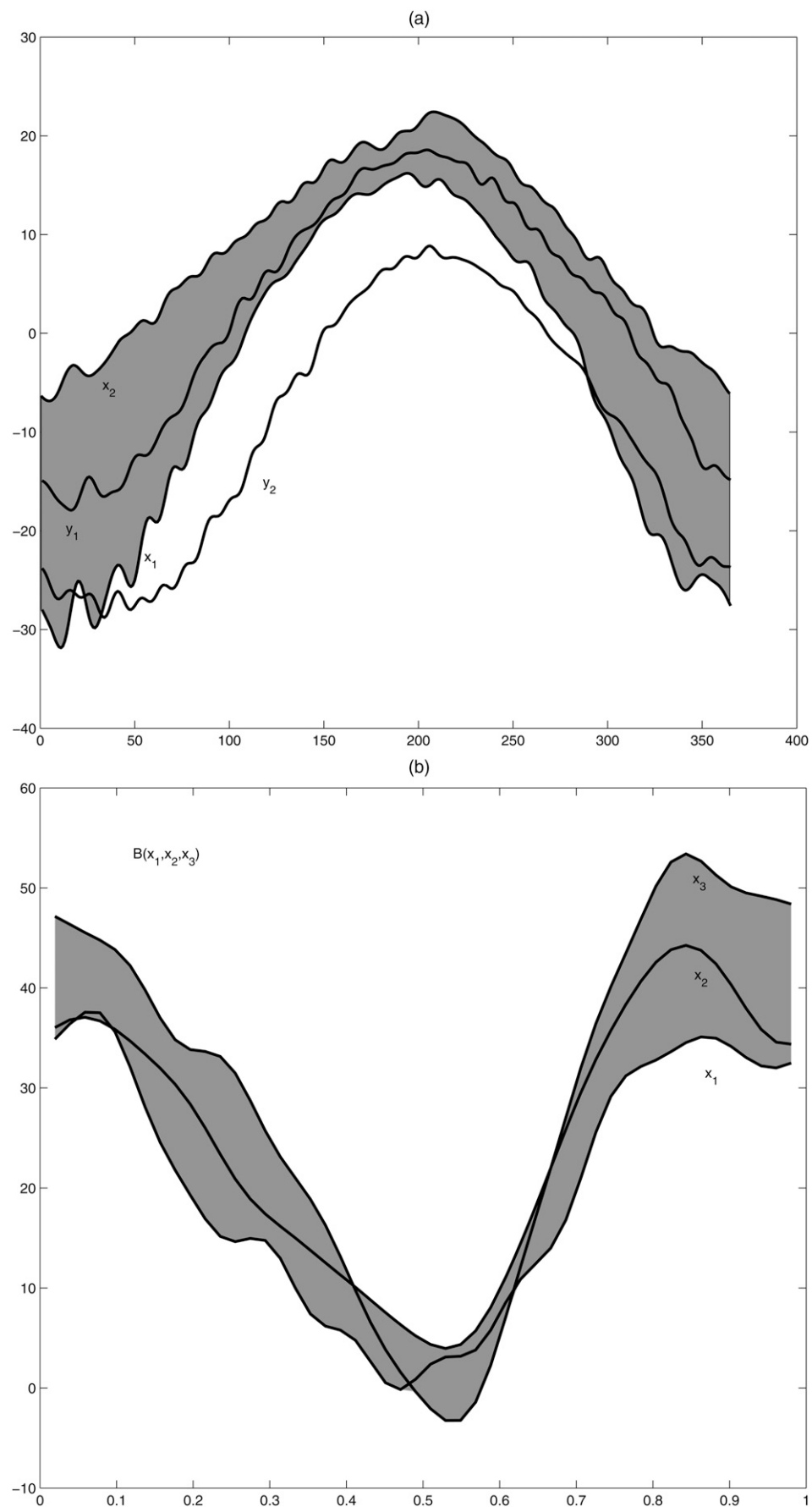


Figure 1. (a) Band defined by two curves x_1 and x_2 . The function y_1 belongs completely to the band, whereas y_2 does not. (b) Band given by three curves x_1 , x_2 , and x_3 .

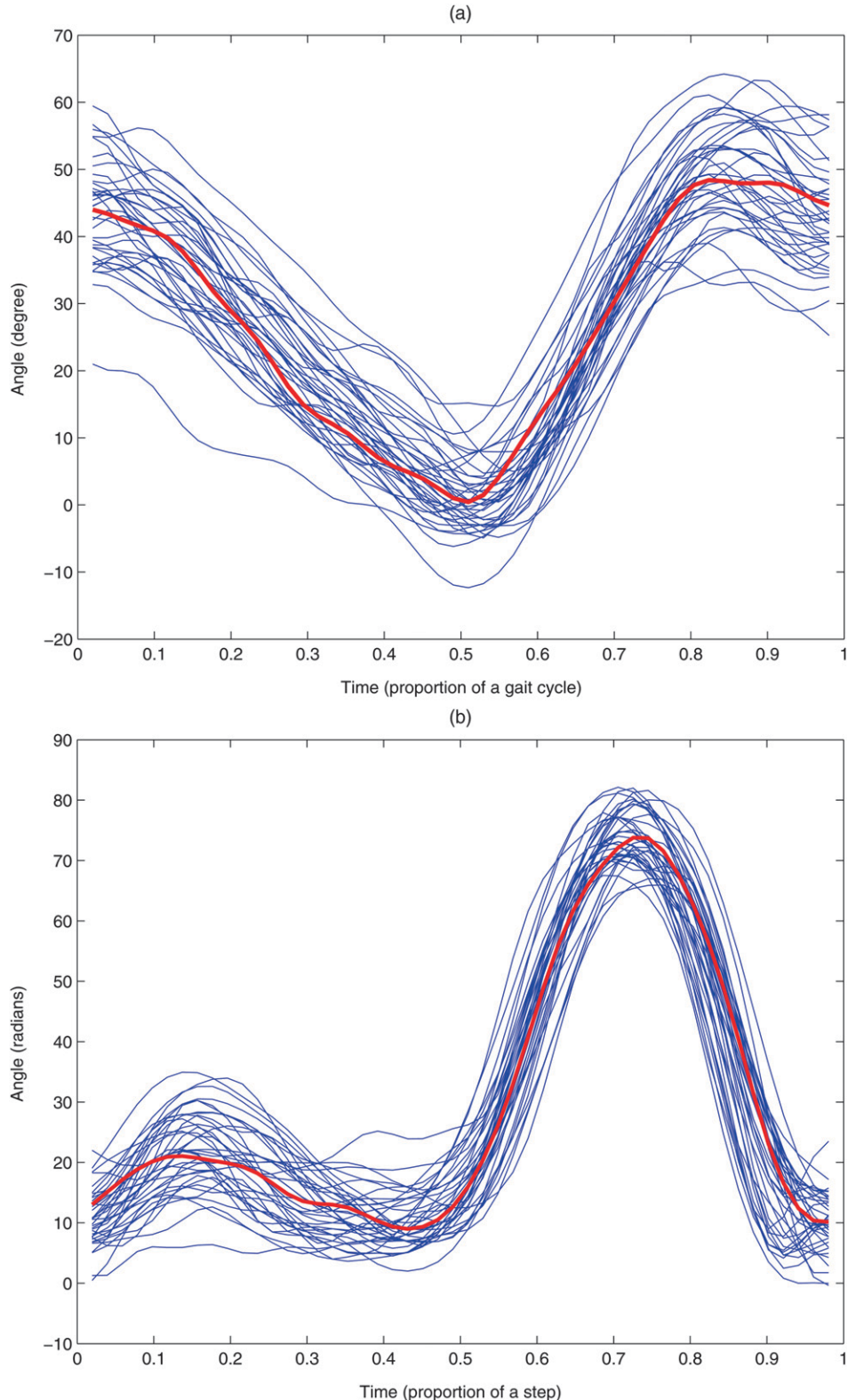


Figure 2. Angle in the sagittal plane formed by (a) the hip and (b) the knee, as 39 children go through a gait cycle. The deepest curves based on BD_n within each sample are represented in red.

An interesting idea that also can be extended to functional data is the concept of α -central region introduced in Liu et al. (1999). It can be defined as the band delimited by the α proportion of deepest curves from the sample. In Figure 3 we represent the sample 0.1—central region for the curves in Figure 2(a).

3. FINITE-DIMENSIONAL VERSION

The finite-dimensional version of the functional band depth provides also a depth for multivariate data. Parallel coordinates (e.g., see Inselberg, 1981, 1985; Inselberg, Reif, and Chomut 1987; Wegman, 1990) are a convenient tool to visualize a set of

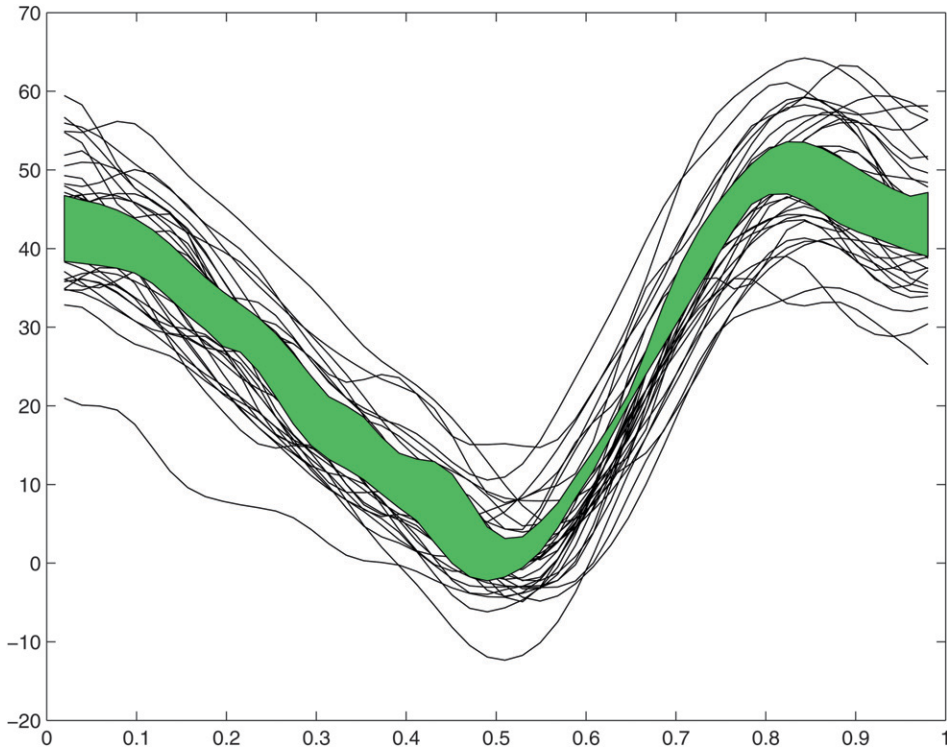


Figure 3. Central region with $\alpha = 0.1$ for the hip curves.

points in \mathbb{R}^d . The cartesian orthogonal axes become parallel and equally spaced in parallel coordinates; thus, points with dimension larger than three can be easily represented. Observations in \mathbb{R}^d can be seen as real functions defined on the set of indexes $\{1, 2, \dots, d\}$ and expressed as $\mathbf{x} = (x(1), x(2), \dots, x(d))$. Given points $\mathbf{x}_1, \mathbf{x}_2, \dots, \mathbf{x}_j$ in \mathbb{R}^d , the corresponding band in parallel coordinates $B(\mathbf{x}_1, \mathbf{x}_2, \dots, \mathbf{x}_j) = \{(k, y) : k \in \{1, 2, \dots, d\}, \min_{i=1, \dots, j} x_i(k) \leq y \leq \max_{i=1, \dots, j} x_i(k)\}$ becomes in cartesian coordinates a d -dimensional interval with sides parallel to the axes delimited by the minimum and the maximum of the coordinates of $\mathbf{x}_1, \mathbf{x}_2, \dots, \mathbf{x}_j$, given by

$$Q(\mathbf{x}_1, \mathbf{x}_2, \dots, \mathbf{x}_j) = \left\{ \mathbf{x} \in \mathbb{R}^d : \min_{i=1, \dots, j} x_i(k) \leq x(k) \leq \max_{i=1, \dots, j} x_i(k) \right\}.$$

Figures 4(a) and 4(b) present the band delimited by three points in the plane in parallel and cartesian coordinates, respectively. For any point \mathbf{x} in $\mathbf{x}_1, \dots, \mathbf{x}_n$, $BD_n^{(j)}(\mathbf{x})$ is the proportion of sets $Q(\mathbf{x}_{i_1}, \mathbf{x}_{i_2}, \dots, \mathbf{x}_{i_j})$ defined by j different points $\mathbf{x}_{i_1}, \mathbf{x}_{i_2}, \dots, \mathbf{x}_{i_j}$ from the sample containing \mathbf{x} . Hence, for points $\mathbf{x}_1, \dots, \mathbf{x}_n$, the band depth of any of these points \mathbf{x} is defined as in Equation (1). The population version for the probability distribution P is analogous to the previous one. As in the functional case, we consider $J = 3$ and denote the population and sample band depth as BD and BD_n . The band depth can be seen as a depth concept in the spirit of simplicial depth (Liu, 1990); instead of simplices, we use rectangles (in particular, d -dimensional intervals), which lead to bands in the functional case.

3.1 Band Depth Properties

The detailed proofs of all properties included in this section can be seen at the website <http://www.uc3m.es/uc3m/dpto/DEE/departamento.html>.

The deepest point for the band depth in one dimension is the usual univariate median. Liu (1990) established natural properties a notion of depth should satisfy. Zuo and Serfling (2000a) analyzed them in a very general framework. Band depth satisfies all these properties except affine invariance. However, this is not a drawback because affine invariance is not a natural requirement for functional data. Our first theorem gives the structural properties of the band depth: monotonicity, maximality at center, vanishing at infinity, and continuity.

Theorem 1. Let P be a probability distribution in \mathbb{R}^d . Then:

- (1) If P is absolutely continuous and its marginals P_i , $i = 1, 2, \dots, d$, are symmetric with respect to m_i then $BD(\alpha(\mathbf{x} - \mathbf{m}))$, $\mathbf{m} = (m_1, \dots, m_d)$, is a monotone nonincreasing function in $\alpha \geq 0$, for all $\mathbf{x} \in \mathbb{R}^d$.
- (2) Under the conditions in (1), if the density f is positive in a neighborhood of the center of symmetry \mathbf{m} then $BD(\cdot)$ is uniquely maximized at \mathbf{m} .
- (3) $\sup_{\|\mathbf{x}\|_\infty \geq M} BD(\mathbf{x}) \rightarrow 0$, as $M \rightarrow \infty$ and $\sup_{\|\mathbf{x}\|_\infty \geq M} BD_n(\mathbf{x}) \xrightarrow{a.s.} 0$, as $M \rightarrow \infty$
- (4) $BD(\cdot)$ is upper-semicontinuous. If the marginal distributions of P are absolutely continuous then $BD(\cdot)$ is continuous.

The monotonicity property in (1) holds under the assumption of symmetric marginal distributions. Some kind of symmetry assumption is common for many notions of depth (e.g., see Liu, 1990). Property (1) guarantees that the contours $\{\mathbf{x} \in \mathbb{R}^d : BD(\mathbf{x}) = c\}$ are nested and move away from the center as c decreases. Contours, trimmed and central regions for different multivariate depths have been extensively studied in the literature

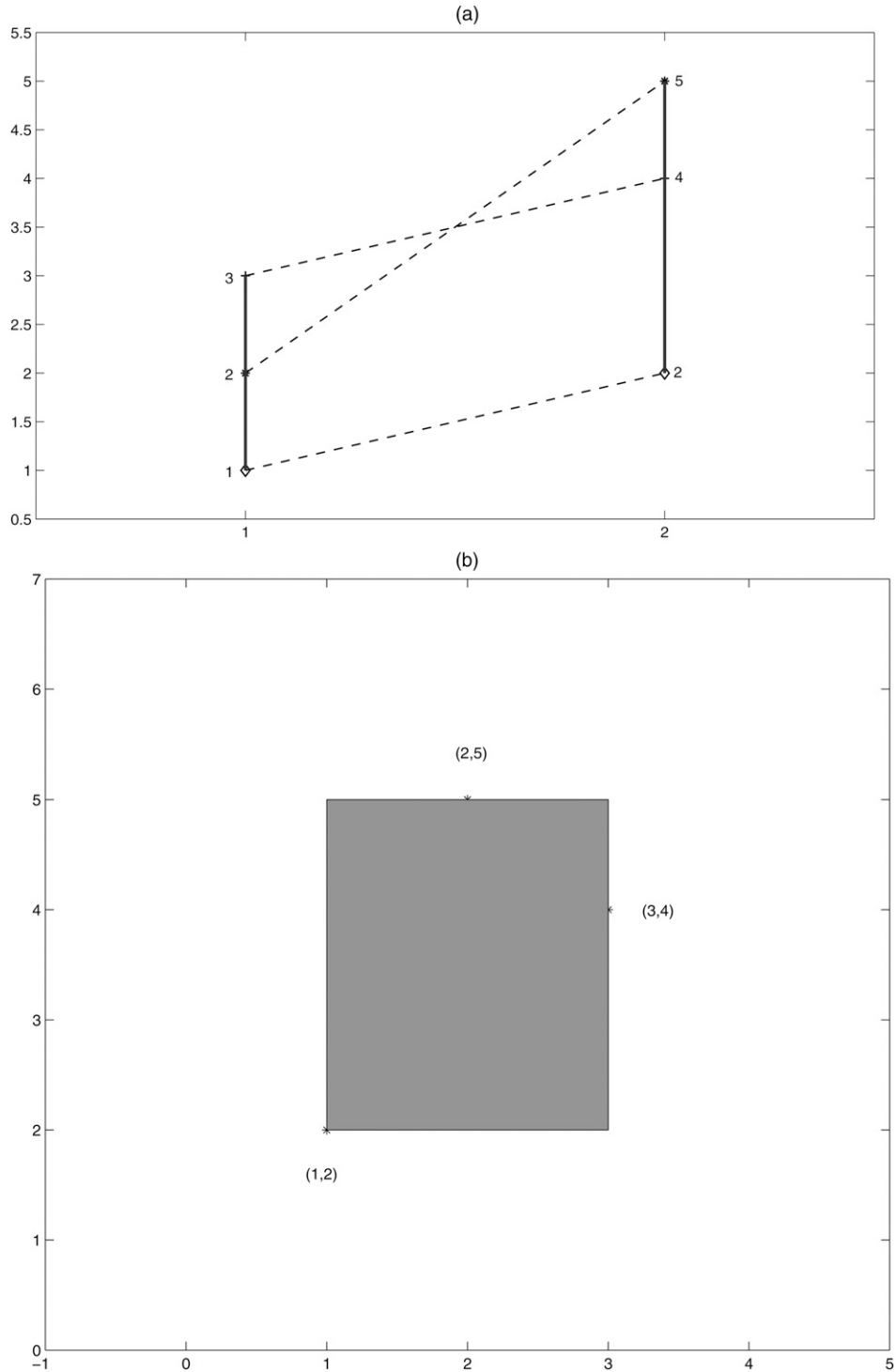


Figure 4. (a) Points $(1, 2)$, $(2, 5)$, and $(3, 4)$ and the corresponding band and (b) the same three points and interval in Cartesian coordinates.

(e.g., see Liu et al. 1999; Zuo and Serfling, 2000b; Mosler, 2002; Zuo, 2003).

The monotonicity in (1) is not necessarily satisfied if the underlying distribution is not absolutely continuous: let $d = 1$, $P(X = 0) = 1/5$, $P(X = \pm 1) = 1/5$, and $P(X = \pm 2) = 1/5$; X is symmetric with respect to 0, $BD_2(1/2; P) = 12/25$, $BD_2(1; P) = 15/25$, and also $BD_3(1/2; P) \leq BD_3(1; P)$.

Several interesting properties follow from the fact that the band depth is a U -statistic.

Proposition 1. $BD_J(x)$ can be expressed as a U -statistic of order J .

The symmetry of P is inherited by the sample distribution of the deepest point. Recall that a variable \mathbf{X} with distribution P is symmetric with respect to \mathbf{c} if $(\mathbf{X} - \mathbf{c})$ and $-(\mathbf{X} - \mathbf{c})$ have the same distribution (e.g., see Liu et al. 1999).

Proposition 2. If P is symmetric then the distribution of the sample deepest point $\hat{\mathbf{m}}_n$ is also symmetric with respect to the population center of symmetry.

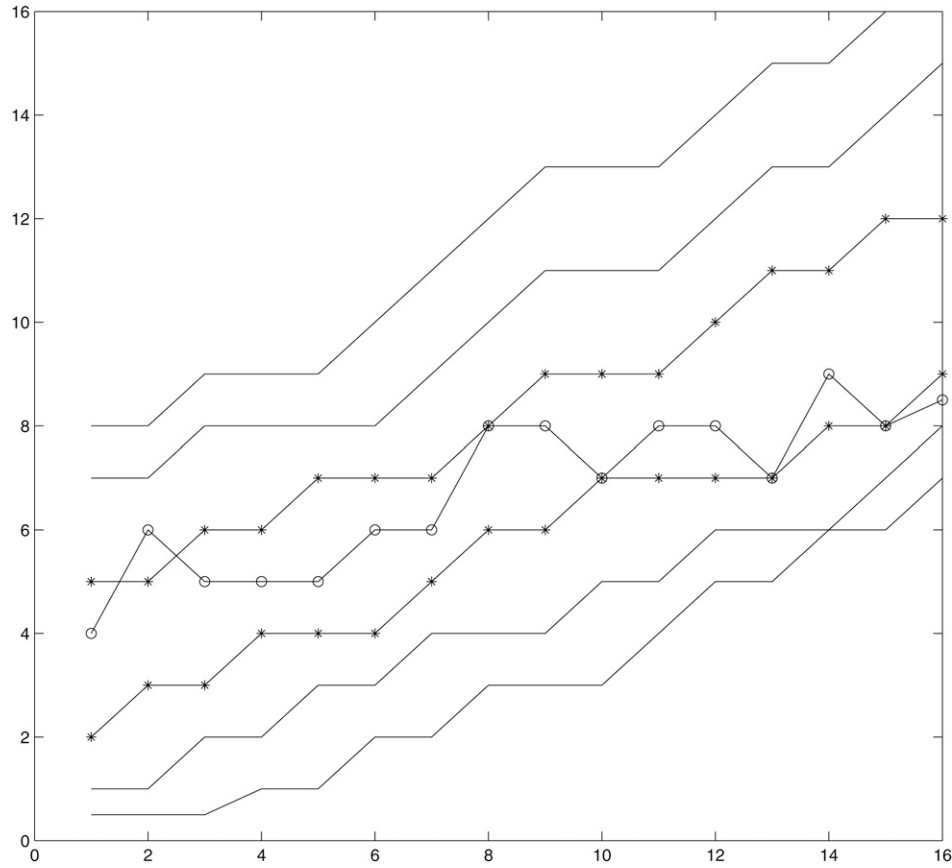


Figure 5. Comparison of deepest curves with band depth and modified band depth.

3.2 Asymptotic Results

Theorem 2 provides the consistency properties of the band depth. Consider $BD_n^{(j)}(\mathbf{x}) = \binom{n}{j}^{-1} \sum_{1 \leq i_1 < \dots < i_j \leq n} I\{\mathbf{x} \in Q(\mathbf{X}_{i_1}, \dots, \mathbf{X}_{i_j})\}$, where \mathbf{X}_i are independent and identically distributed random variables taking values in \mathbb{R}^d with distribution P and $Q(\mathbf{X}_1, \dots, \mathbf{X}_j)$ is the closed interval in \mathbb{R}^d defined by the random points $\mathbf{X}_1, \dots, \mathbf{X}_j$. Following notation in Arcones and Giné (1993), $BD_n^{(j)}(\mathbf{x})$ is a U -process of order j indexed by the class of functions $F = \{Q_\mathbf{x}: \mathbf{x} \in \mathbb{R}^d\}$, where $Q_\mathbf{x} = \{I\{(\mathbf{x}_1, \dots, \mathbf{x}_j): \mathbf{x} \in Q(\mathbf{x}_1, \dots, \mathbf{x}_j)\}\}$. Then $BD_n^{(j)}(\mathbf{x}) = U_j^n(Q_\mathbf{x})$ and its population version is $BD^{(j)}(\mathbf{x}) = P^j(\mathbf{x} \in Q(\mathbf{X}_1, \dots, \mathbf{X}_j))$.

Theorem 2. Let P be a probability distribution in \mathbb{R}^d . Then:

- (1) $\sup_{\mathbf{x} \in \mathbb{R}^d} |BD_n(\mathbf{x}) - BD(\mathbf{x})| \xrightarrow{a.s.} 0$, as $n \rightarrow \infty$.
- (2) If $BD(\cdot)$ is maximized at \mathbf{m} , and \mathbf{m}_n is a sequence of random variables such that $BD_n(\mathbf{m}_n) = \sup_{\mathbf{x} \in \mathbb{R}^d} BD_n(\mathbf{x})$ then $\mathbf{m}_n \xrightarrow{a.s.} \mathbf{m}$, as $n \rightarrow \infty$.
- (3) (Consistency of the sample deepest point) If the density f is different from zero in a neighborhood of \mathbf{m} and $BD(\cdot)$ is uniquely maximized at \mathbf{m} then $\hat{\mathbf{m}}_n \xrightarrow{a.s.} \mathbf{m}$, as $n \rightarrow \infty$.

Longitudinal data defined on discrete time values $t = 1, 2, \dots, T$ are a particular case of finite-dimensional observations: all the definitions and properties presented in this section can be applied to this type of data.

4. PROPERTIES OF THE FUNCTIONAL BAND DEPTH

Next, we analyze the band depth properties for functions. Let X be a process in $C(I)$ with a tight distribution P_X [i.e., $P(\|X\|_\infty \geq M) \rightarrow 0$, as $M \rightarrow \infty$ (see Pollard, 1984)]. The following results give the basic properties of the functional depth BD .

Theorem 3. (1) Let $T(x) = ax + b$, where x , a , and b are continuous functions in I , with $a(t) \neq 0$ for each $t \in I$. Then $BD(x, P_X) = BD(ax + b, P_{aX+b})$, where P_{aX+b} is the probability distribution of the transformed random process $aX + b$. Moreover, $BD(x, P_X) = BD(h(x), P_{h(X(\cdot))})$, where h is a strictly monotone transformation of the function values.

(2) $BD(x(t), P_X) = BD(x(g(t)), P_{X(g(t))})$, where g is a one-to-one transformation of the interval I .

(3) $\sup_{\|x\|_\infty \geq M} BD(x) \longrightarrow 0$ and $\sup_{\|x\|_\infty \geq M} BD_n(x) \xrightarrow{a.s.} 0$, as $M \rightarrow \infty$.

(4) BD is an upper-semicontinuous function. Moreover, if the probability distribution P on $C(I)$ has absolutely continuous marginal distributions, then the band depth BD is a continuous functional on $C(I)$.

Recall that a random variable X on $C(I)$ is symmetric (with respect to zero) if X and $-X$ have the same distribution.

Proposition 3. If the population random variable X on $C(I)$ is symmetric then the distribution of $\hat{\mathbf{m}}_n$ is also symmetric.

The band depth is uniformly consistent on compact sets of functions.

Theorem 4. Let P be a probability distribution on $C(I)$ with absolutely continuous marginal distributions. Then,

(1) $BD_n(\cdot)$ is uniformly consistent on any equicontinuous set E , i.e.,

$$\sup_{x \in E} |BD_n(x) - BD(x)| \xrightarrow{a.s.} 0, \text{ as } n \rightarrow \infty.$$

(2) If $BD(\cdot)$ is uniquely maximized at $m \in E$, and m_n is a sequence of functions in E with $BD_n(m_n) = \sup_{x \in E} BD_n(x)$ then $m_n \xrightarrow{a.s.} m$, as $n \rightarrow \infty$.

For instance, the set $Lip_{\alpha,A}(I) = \{x : I \rightarrow \mathbb{R}, |x(t_1) - x(t_2)| \leq A|t_1 - t_2|^\alpha, t_1, t_2 \in I\}$ is equicontinuous and satisfies the condition in Theorem 4; hence, BD_n converges uniformly to BD over $Lip_{\alpha,A}(I)$. The usual Lipschitzian functions are a particular case of $Lip_{\alpha,A}(I)$ (with $\alpha = 1$) and thus the band depth is uniformly consistent on the Lipschitz functions.

5. A MODIFIED BAND DEPTH

Instead of considering the indicator function, a more flexible definition can be introduced by measuring the set where the function is inside the corresponding band. For any of the functions x in x_1, \dots, x_n and for $2 \leq j \leq n$, let

$$\begin{aligned} A_j(x) &\equiv A(x; x_{i_1}, x_{i_2}, \dots, x_{i_j}) \equiv \left\{ t \in I : \min_{r=i_1, \dots, i_j} x_r(t) \leq x(t) \right. \\ &\quad \left. \leq \max_{r=i_1, \dots, i_j} x_r(t) \right\} \end{aligned}$$

be the set in the interval I where the function x is in the band determined by the observations $x_{i_1}, x_{i_2}, \dots, x_{i_j}$. If λ is the Lebesgue measure on I , $\lambda_r(A_j(x)) = \lambda(A_j(x))/\lambda(I)$ gives the “proportion of time” that x is in the band. Now,

$$MBD_n^{(j)}(x) = \binom{n}{j}^{-1} \sum_{1 \leq i_1 < i_2 < \dots < i_j \leq n} \lambda_r(A(x; x_{i_1}, x_{i_2}, \dots, x_{i_j})), \quad 2 \leq j \leq n$$

is a more flexible version of $BD_n^{(j)}(x)$: if x is always inside the band, the value $\lambda_r(A_j(x))$ is one as in the previous notion of depth.

Definition 2. Let J be a fixed value with $2 \leq J \leq n$. For functions x_1, \dots, x_n , the *modified band depth* of any of these curves x is

$$MBD_{n,J}(x) = \sum_{j=2}^J MBD_n^{(j)}(x).$$

The population version of the modified band depth is $MBD_J(x) = \sum_{j=2}^J MBD^{(j)}(x)$, where $MBD^{(j)}(x) = E \lambda_r(A(x; X_1, X_2, \dots, X_j))$.

In the finite-dimensional case, the value $MBD_n^{(j)}(\mathbf{x})$ is defined as the proportion of coordinates of \mathbf{x} inside the interval given by j different points from the sample:

$$\begin{aligned} MBD_n^{(j)}(\mathbf{x}) &= \binom{n}{j}^{-1} \sum_{1 \leq i_1 < \dots < i_j \leq n} \frac{1}{d} \sum_{k=1}^d I\{\min\{x_{i_1}(k), \dots, \\ &\quad x_{i_j}(k)\} \leq x(k) \leq \max\{x_{i_1}(k), \dots, x_{i_j}(k)\}\}, \end{aligned}$$

and then

$$MBD_{n,J}(\mathbf{x}) = \sum_{j=2}^J MBD_n^{(j)}(\mathbf{x}).$$

It is straightforward to check that in the univariate case ($d = 1$) the band depth and the modified band depth coincide. Moreover, the ordering induced by these depths when $d = 1$ does not depend on J . Throughout the article we will consider the modified band depth with $J = 2$ (denoted as MBD) because it is computationally fast, the order induced is very stable in J , and (contrary to the band depth) it will provide reasonable orders even if many curves from the sample cross over. If $SD_{F_{n,k}}(x(k))$ is the univariate simplicial depth of $x(k)$, then

$$\begin{aligned} MBD_n(\mathbf{x}) &= \frac{1}{d} \sum_{k=1}^d \binom{n}{2}^{-1} \sum_{1 \leq i_1 < i_2 \leq n} I\{\min\{\mathbf{x}_{i_1}(k), \mathbf{x}_{i_2}(k)\} \\ &\quad \leq \mathbf{x}(k) \leq \max\{\mathbf{x}_{i_1}(k), \mathbf{x}_{i_2}(k)\}\} \\ &= \frac{1}{d} \sum_{k=1}^d SD_{F_{n,k}}(\mathbf{x}(k)); \end{aligned}$$

hence, from the simplicial depth properties (see Liu, 1990), it is straightforward to prove that the finite-dimensional version of the modified band depth satisfies the properties in Theorem 1 [except (3)] and the consistency results in Theorem 2. Property (3) in Theorem 1 can be seen as being too strict for functional data: even for multivariate data, Zuo and Serfling (2000a) proposed some weaker variants of the property.

The band depth is more dependent on the curves shape and more restrictive than the modified version, providing frequent ties (several curves with the same depth). The modified band depth relies more on the magnitude or size of the curves than on

Table 1. Mean integrated squared errors using as location estimators the mean, the trimmed mean based on (BD) , (MBD) , (FM) , (L_1D) , and (C) for models 1–4 with 500 replications, 50 curves, $\alpha = 0.2$, $q = 0.1$, and contamination constant $K = 25$.

Const.	Est.	Model 1	Model 2	Model 3	Model 4
$K = 25$	mean	0.0207 (0.0065)	1.1394 (1.4477)	0.6176 (0.7046)	0.1479 (0.0844)
	BD	0.0262 (0.0082)	0.4222 (1.2920)	0.7199 (0.8452)	0.0981 (0.0777)
	MBD	0.0274 (0.0079)	0.0297 (0.0360)	0.0473 (0.0439)	0.1817 (0.1103)
	FM	0.0263 (0.0079)	0.0303 (0.0409)	0.0545 (0.0613)	0.1822 (0.1079)
	L_1D	0.0264 (0.0080)	0.0304 (0.0358)	0.0272 (0.0117)	0.0254 (0.0268)
	C	0.0215 (0.0050)	0.0811 (0.3153)	0.0371 (0.0710)	0.0211 (0.0205)

NOTE: Standard errors are given in parenthesis.

Table 2. Mean integrated squared errors using as location estimators the mean, the trimmed mean based on (BD), (MBD), (FM), (L_1D) and (C) for models 5–8 with 500 replications, 50 curves, $\alpha = 0.2$, and contamination probability $q = 0.1$.

	Est.	Model 5 $\mu_2 = 0.2$ $k_2 = 1$	Model 6 $\mu_2 = 0.1$ $k_2 = 2$	Model 7 $\mu_2 = 0.2$ $k_2 = 2$	Model 8 $\mu_2 = 0.3$ $k_2 = 2$
$q = 0.1$	mean	0.031 (0.0314)	0.0459 (0.0548)	0.0724 (0.0715)	0.0441 (0.0453)
	BD	0.027 (0.0301)	0.0292 (0.0417)	0.0391 (0.0437)	0.0276 (0.0321)
	MBD	0.0362 (0.0353)	0.0434 (0.0571)	0.0644 (0.0679)	0.0402 (0.0422)
	FM	0.0391 (0.0385)	0.0479 (0.0564)	0.0711 (0.0748)	0.0449 (0.0481)
	L_1D	0.0312 (0.0324)	0.0310 (0.0445)	0.0452 (0.0525)	0.0298 (0.0333)
	C	0.0300 (0.0295)	0.0350 (0.0443)	0.0516 (0.0546)	0.0336 (0.0339)

NOTE: Standard errors are given in parenthesis.

their shape. Another relevant difference between them is their behavior for curves leaving the center of the sample only for a short interval (i.e., remaining in the interior of the sample almost all of the time, but taking extreme values in short subintervals): the modified band depth can still be large for them but the band depth will always take small values on these curves. The functions in Figure 5 illustrate these differences: all of them are increasing, except the one with circles, which is more irregular and not increasing. The deepest curves with BD are the ones with asterisks, whereas the deepest curve for the modified band depth is the one with circles. The deepest curves for the band depth resemble the sample functions. The deepest curve for the modified depth is different in shape but turns out to be the closest in L_2 distance to the mean: thus, band depth is shape sensitive. Using the band depth or the modified band depth depends on the kind of functions being analyzed and the study goal. If the curves are very irregular, it is convenient to use the modified band depth because it avoids having too many depth ties and there might not be a representative “shape”; however, the band depth is more adequate if the curves are smooth and the goal is the most representative curve in terms of shape (not magnitude).

6. SIMULATION RESULTS

In contrast to most of the previous definitions of depth, the band depth and the modified band depth are not computationally intensive. This makes them convenient for analyzing very high-dimensional data. We have generated 100 simulations of 50 points from a bivariate normal distribution with mean zero and covariance matrix the identity. The average empirical central processing unit (CPU) time to compute simplicial, halfspace, band, and modified band depths are 82.10, 5.76, 1.98, 0.35 s, respectively. In higher dimensions, band and modified band depth are still computationally feasible, whereas simplicial and halfspace depth are not.

6.1 Models

There is no general definition of outlier for functional data. A curve could be an outlier for many reasons: it can be very distant from the mean (magnitude outlier) or have a pattern different from the other curves [e.g., being decreasing when the remaining ones are increasing or very irregular in a set of smooth curves (shape outlier)]. In general, we consider that a curve is an outlier if it comes from a different process than the

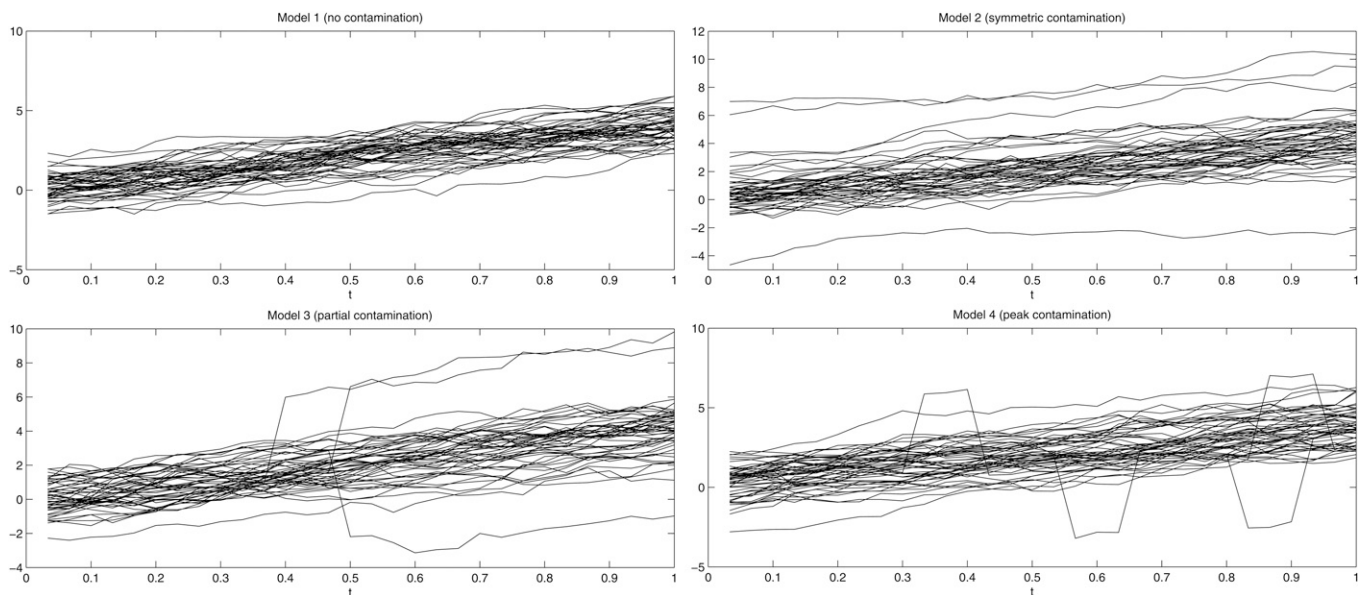


Figure 6. Curves generated from model 1 (without contamination), model 2 (symmetric contamination), model 3 (partial contamination), and model 4 (peak contamination).

remaining curves. Thus, robust location estimates are important in functional data analysis.

We have generated curves from different models: a basic one without contamination (model 1) and several models with different types of contamination. The first three contaminated models (represented in Table 1 as model 2 to model 4) have magnitude outliers (some of these models were already considered in Fraiman and Muniz, 2001). The four models included in Table 2 (model 5 to model 8) have shape contaminations.

Magnitude contamination: The basic model 1 is $X_i(t) = g(t) + e_i(t)$, $1 \leq i \leq n$, with mean $g(t) = 4t$, $t \in [0, 1]$, and where $e_i(t)$ is a stochastic Gaussian process with zero mean and covariance function $\gamma(s, t) = \exp\{-|t - s|\}$.

Model 2 includes a symmetric contamination: $Y_i(t) = X_i(t) + c_i \sigma_i K$, $1 \leq i \leq n$, where c_i is 1 with probability q and 0 with probability $1 - q$, K is a contamination size constant and σ_i is a sequence of random variables independent of c_i taking values 1 and -1 with probability $1/2$.

Model 3 is partially contaminated: $Y_i(t) = X_i(t) + c_i \sigma_i K$, if $t \geq T_i$, $1 \leq i \leq n$, and $Y_i(t) = X_i(t)$, if $t < T_i$, where T_i is a random number generated from a uniform distribution on $[0, 1]$.

Model 4 is contaminated by peaks: $Y_i(t) = X_i(t) + c_i \sigma_i K$, if $T_i \leq t \leq T_i + l$, $1 \leq i \leq n$, and $Y_i(t) = X_i(t)$, if $t \notin [T_i, T_i + l]$, where $l = 2/30$ and T_i is a random number from a uniform distribution in $[0, 1 - l]$.

Curves simulated from these four models can be seen in Figure 6.

Shape contamination: Besides magnitude contamination, we have also considered shape contamination. These are outliers that have a different pattern from the other curves, but they are not necessarily far away from the mean in terms of distance. To generate shape outliers, we use a family of models having covariance $\gamma(s, t) = k \exp\{-c|t - s|^\mu\}$, with $s, t \in [0, 1]$, and $k, c, \mu > 0$ (see Wood and Chan, 1994). Parameters k , c , and μ control shape: for example, increasing μ and k , the generated curves are smoother; however, by increasing c , the generated functions are more irregular. We have considered a set of shape contaminated models (model 5 to model 8) defined as a mixture of a basic model $X_i(t) = g(t) + e_{1i}(t)$, $1 \leq i \leq n$, with $g(t) = 4t$ and $e_{1i}(t)$ a Gaussian stochastic process with zero mean and covariance function $\gamma_1(s, t) = \exp\{-|t - s|^2\}$ and $Y_i(t) = g(t) + e_{2i}(t)$, $1 \leq i \leq n$, where $e_{2i}(t)$ is a Gaussian process with zero mean and covariance function γ_2 with values k_2 , c_2 , and μ_2 chosen to generate more irregular curves (for example, in model 5, $\mu_2 = 0.2$, $c_2 = 1$, and $k_2 = 1$). The contaminated models are given by $Z_i(t) = (1 - \varepsilon)X_i(t) + \varepsilon Y_i(t)$, $1 \leq i \leq n$, where ε is a Bernoulli variable $Be(q)$ and q is a small contamination probability; thus, we contaminate a sample of smooth curves from $X_i(t)$ with curves from $Y_i(t)$ having different covariance functions and providing more irregular curves. Figure 7 shows curves simulated from model 5: the contaminated curves behave more irregularly than the remaining functions, but they are not far from them in terms of distance.

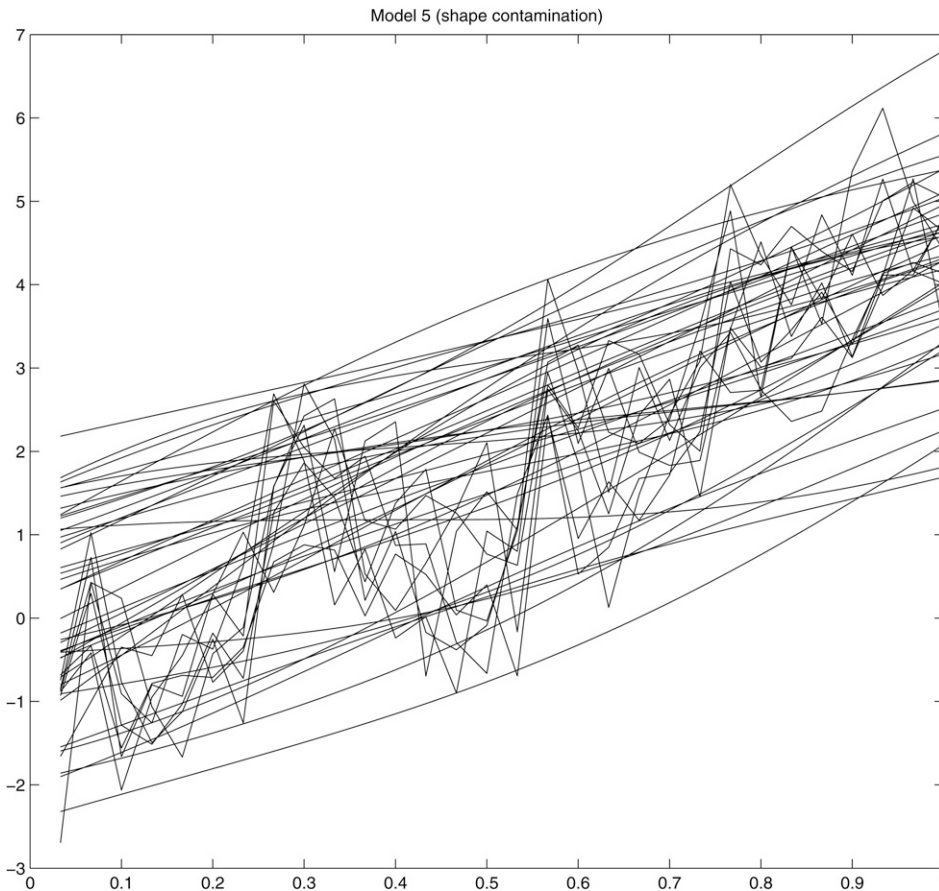


Figure 7. Curves from model 5 with $k_2 = c_2 = 1$, $\mu_2 = 0.2$ and contamination probability $q = 0.1$.

Table 3. Percentage of times that an outlier is detected with 100 replications, 50 curves, and $\alpha = 0.2$.

$\mu_2 = 0.1 k_2 = 1$	$\mu_2 = 0.2 k_2 = 1$	$\mu_2 = 0.3 k_2 = 1$	$\mu_2 = 0.1 k_2 = 2$	$\mu_2 = 0.2 k_2 = 2$	$\mu_2 = 0.3 k_2 = 2$
<i>BD</i>	100	100	100	100	100
<i>MBD</i>	18	13	24	23	35
<i>FM</i>	14	10	20	15	21
<i>L₁D</i>	57	47	53	65	96

6.2 Simulation Results

We analyze the robustness of statistics based on functional depth for the previous models. We compare the mean and the coordinate-wise α -trimmed mean with the depth based α -trimmed mean, given by

$$\hat{m}_n^\alpha(t) = \sum_{i=1}^{n-[n\alpha]} x_{(i)}(t)/(n - [n\alpha]),$$

where $x_{(1)}, x_{(2)}, \dots, x_{(n)}$ is the sample ordered from the deepest to the least deep curve and $[n\alpha]$ is the integer part of $n\alpha$. Four notions of depth are used: *BD*, its modified version *MBD*, *FM* (Fraiman and Muniz's depth), and *L₁D* (Vardi and Zhang's depth). For each model, we have considered 500 replications, generating $n = 50$ curves in each replication, contamination probability $q = 0.1$, contamination constant $K = 25$, and $\alpha = 0.2$. The integrated squared error evaluated at $T = 30$ equally spaced points in $[0, 1]$ for each replication j is

$$ISE(j) = \frac{1}{T} \sum_{k=1}^T [\hat{g}_n(k/T) - g(k/T)]^2,$$

where \hat{g}_n is the corresponding location estimator. Table 1 contains the mean integrated squared error for models 1–4. As

expected, in the model without contamination, the mean behaves always better than the trimmed means. For model 2, all trimmed means outperform the mean. In model 3, all trimmed means, except *BD*, behave better than the mean. However, in model 4 the trimmed mean based on *BD* has smaller mean integrated squared error than the mean. Thus, for these magnitude contaminated models there is no estimator outperforming all the others.

Table 2 contains the simulation results for the family of shape contaminated models with 500 replications, $n = 50$ curves, $\alpha = 0.2$, and contamination probability $q = 0.1$. We have considered different values of μ_2 and k_2 to modify the covariance of $Y(t)$ ($c_2 = 1$ in all cases). As with previous models, we compare the mean, the coordinate-wise trimmed mean, and the depth based trimmed means in terms of robustness. The mean integrated squared error using the different location estimators are represented for each shape contamination model (model 5 to model 8). The minimum mean integrated squared error corresponds always to the trimmed mean based on the band depth *BD*. This is due to the contamination type: shape more than magnitude. Thus, the band depth performs well in terms of robustness with respect to this kind of outliers. However, the trimmed means based on other depths and the coordinate-wise trimmed mean are less robust

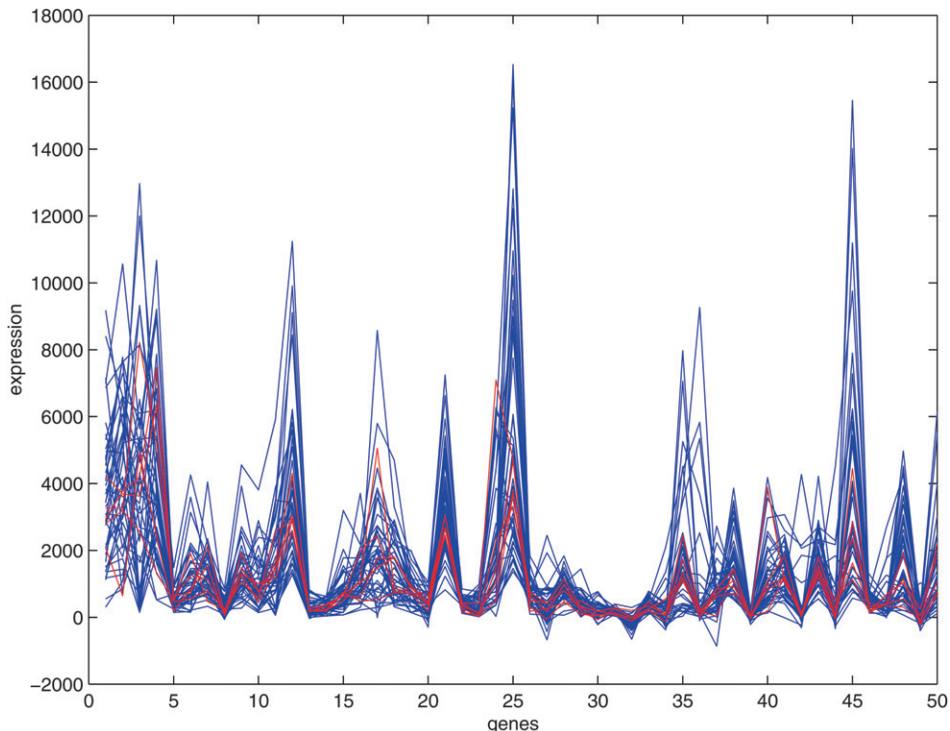


Figure 8. Expression of 50 genes for 47 individuals with lymphoblastic leukemia. The five deepest curves are represented in red.

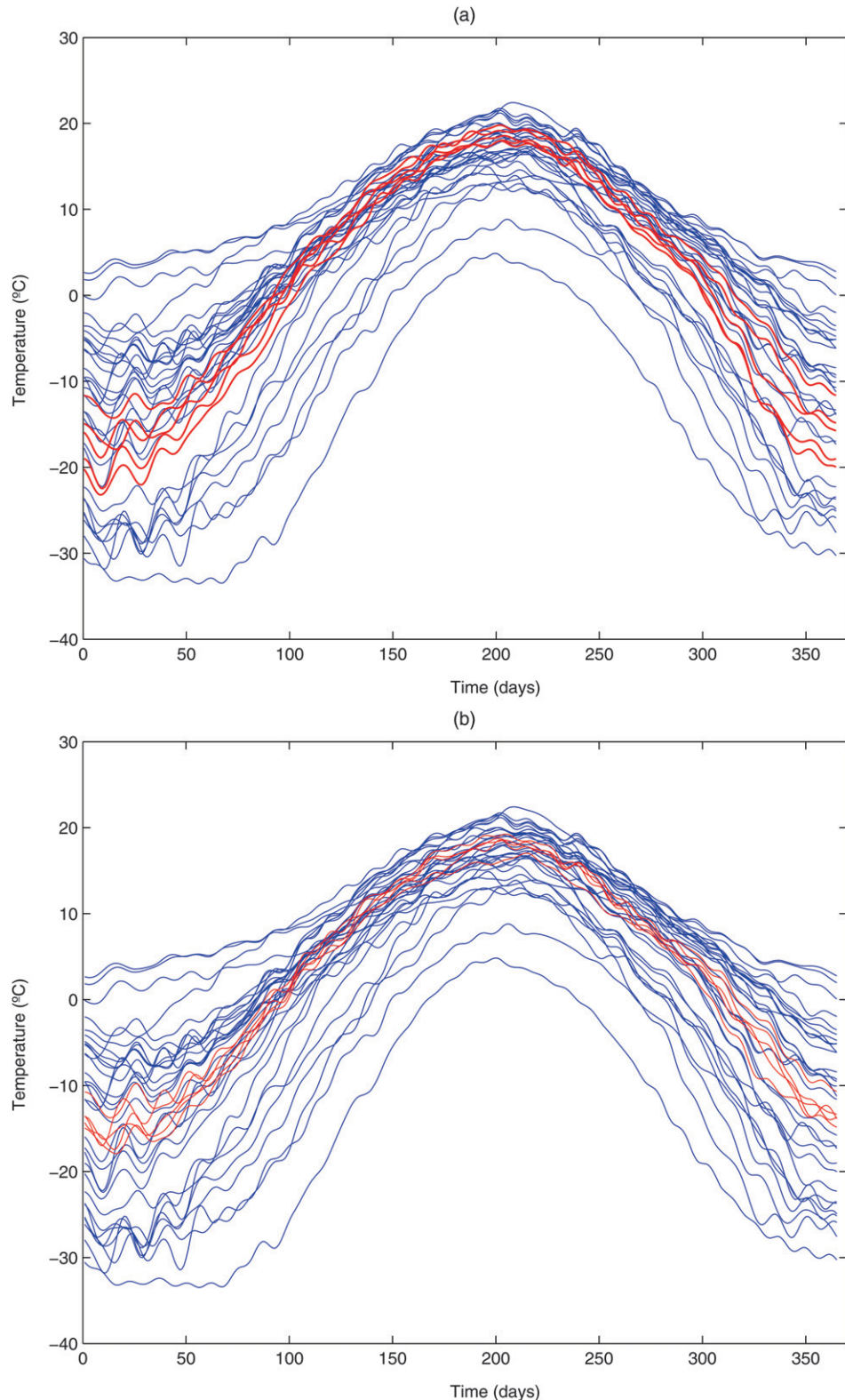


Figure 9. Daily temperature in 35 Canadian weather stations for one year. The five deepest curves (in red) based on (a) *BD* and (b) *MBD*.

against shape contamination, because most of the contaminated curves values can still be very central in the sample (in terms of distance), although the curve behavior is different from the remaining functions. Therefore, when there is shape contamination in the data, the most robust procedure is based on

the band depth because it will assign low depth to curves with a different shape.

Besides providing a location estimator, the idea of depth can also be a useful tool for detecting outliers when analyzing functional datasets. Recall that functional depth provides a

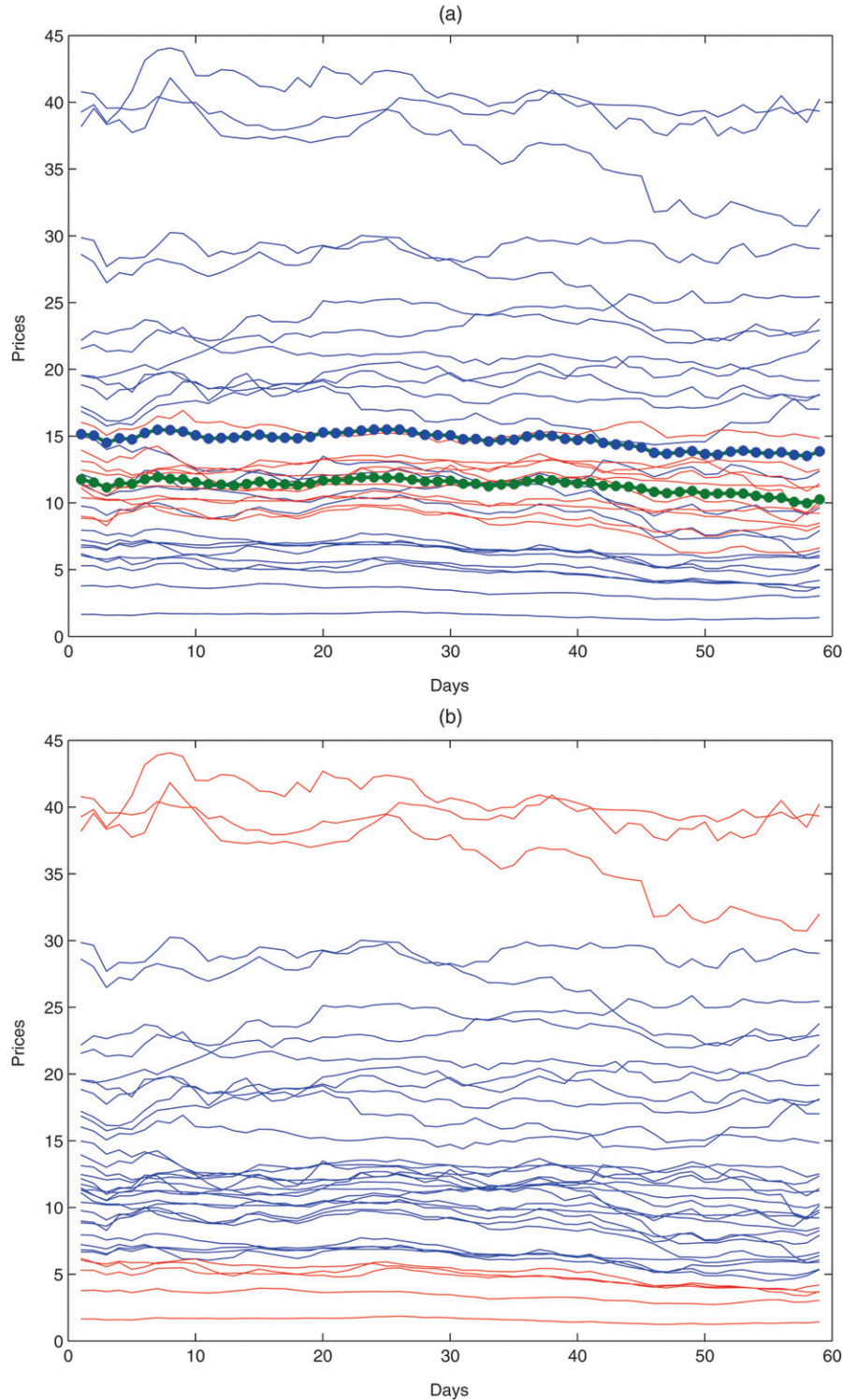


Figure 10. Prices included in the IBEX 35 index. (a) The 30% deepest curves are in red, and mean and median are marked with blue and green asterisks, respectively. (b) The 25% most extreme curves appear in red.

center-outward ordering of the set of curves. The curve (or curves) with maximum depth can be used to estimate the location or center of this set of curves, and functions with low depth can be considered outliers or extreme observations.

We have compared the shape outlier detection performance of the different notions of depth in contamination settings similar to those in Table 2. We simulated 49 curves from the basic model X and one curve from the contaminated model Y

using different values of the parameters μ_2 and k_2 . We replicated the simulation 100 times and counted the number of times the outlying curve is within the 20% least deepest curves from the sample. The results depend strongly on the notion of depth used. For the band depth BD , the outlier was detected 100% of the times, whereas for the other notions of depth this percentage varies but was always lower than 100 (see Table 3). Detecting shape contaminated curves is not an easy task: the

band depth performed significantly better compared with the other functional depths.

7. REAL DATA EXAMPLES

7.1 High-Dimensional Data Example: Application to Microarray Data

An important advantage of band depths is that they can be applied to high-dimensional data with low computational cost. This contrasts with most of the multivariate depths introduced in the literature, which are computationally intensive. For instance, simplicial depth (Liu, 1990) and halfspace depth (Tukey, 1975) are not feasible when the dimension of the data are greater than three. This is a critical limitation to analyze complex or high-dimensional data. A particularly attractive application of the novel notions of depth presented in this article relates with the analysis of microarray data. This is a recently developed biotechnology used to measure the level of expression of thousands of genes simultaneously. The data obtained in microarray experiments are considered of high dimension because they present many variables (genes) in relation with the number of observations or tissues (samples). In this high-dimensional context, outliers are difficult to visualize and detect, so robust statistics are essential for the analysis. An example of microarray data is shown in Figure 8 where the level of expression of 50 genes in a sample of 47 individuals with acute lymphoblastic leukemia is represented using parallel coordinates. To illustrate a preliminary first approach to

the depth-based analysis that can be performed in this example, we have calculated the five more representative (or deepest) expression profiles (curves in red) using the modified band depth. Based on the center-outward sample order provided by the notion of depth, we can define the median or trimmed mean profile and use these location estimates as a starting point for the extension of robust statistical procedures to microarray data.

7.2 Functional Data Examples

The first real functional dataset describes daily temperature in different Canadian weather stations (Ramsay and Silverman, 2005). The original data were smoothed using a Fourier basis with 65 elements. Figure 9(a) shows the temperature curves; the five deepest functions for the band depth are in red. Figure 9(b) presents the five deepest curves using the modified band depth. The second example contains the price curves for the 35 firms in the Spanish IBEX 35 index. The functions include 59 daily measurements starting June 22, 2002. Figure 10(a) gives in red the 30% deepest elements for BD . The mean curve is represented with blue dots and the trimmed mean with $\alpha = 0.3$ appears in green dots. The mean curve is more sensitive to the extreme functions than the trimmed one. In Figure 10(b) the 25% most extreme (least deep) curves from the sample are in red.

8. A RANK TEST FOR FUNCTIONS

These new depth definitions are useful tools for extending standard robust statistics to functional data. For instance, in

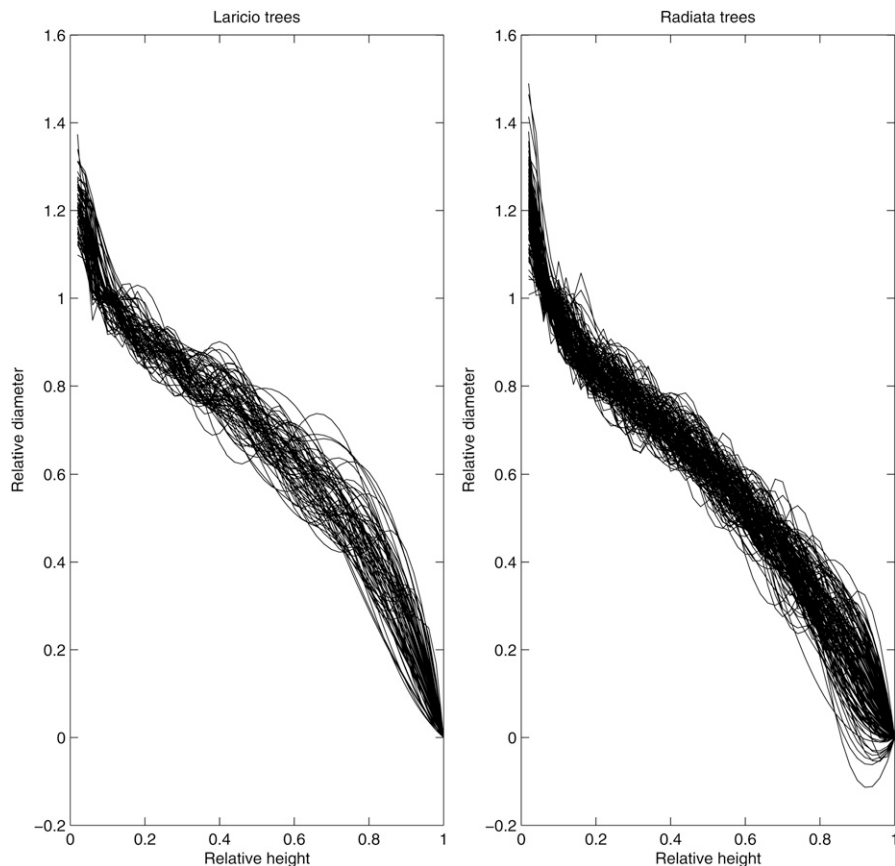


Figure 11. Relative diameter versus relative height for Laricio trees (left panel) and for Radiata trees (right panel).

López-Pintado and Romo (2005) a depth-based classification method for functional data was proposed. The depth definitions for curves also allow us to extend the rank test to functional data. Liu and Singh (1993) generalized to multivariate data the univariate Wilcoxon rank test through the order induced by a multivariate depth. In Mosler (2002) a depth-based rank test for detecting difference in scale and location is described. Brown and Hettmansperger (1989) and Hettmansperger and Oja (1994) have also proposed different rank tests for multivariate observations. Following Liu and Singh (1993), let

$$\begin{aligned} R(P_n, x_i) &= R(x_i) \\ &= \text{proportion of } x_j \text{'s from the sample with } BD_n(x_j) \\ &\leq BD_n(x_i). \end{aligned} \quad (6)$$

It takes values between 0 and 1. We rank the observations x_i according to the increasing values of R , assigning them an integer from 1 to n . If there are curves with the same value of R , $R(x_{i_1}) = R(x_{i_2}) = \dots = R(x_{i_j})$, with $i_1 < i_2 < \dots < i_j$, we consider the rank of $x_{i_{k+1}}$ as the rank of x_{i_k} plus one. We propose a test based on these ranks to decide if two groups of curves come from the same population. Let x_1, \dots, x_n be a sample of curves from population P_1 and let y_1, \dots, y_m be a sample of curves from population P_2 . Assume that there is a third reference sample $Z = \{z_1, z_2, \dots, z_{n_0}\}$ from one of the two populations, for example P_1 , with n_0 greater than n and m . Let P_{n_0} be the corresponding empirical distribution. Calculate

$R(P_{n_0}, x_i) = \text{proportion of } z_j \text{'s with } BD(z_j, P_{n_0}) \leq BD(x_i, P_{n_0})$, and $R(P_{n_0}, y_i) = \text{proportion of } z_j \text{'s with } BD(z_j, P_{n_0}) \leq BD(y_i, P_{n_0})$, that express the position of each x_i and y_i with respect to Z . Order these values, $R(P_{n_0}, X_i)$ and $R(P_{n_0}, Y_i)$, from smallest to highest giving them a rank from 1 to $n + m$. If there are ties, we apply the previous criterion. The proposed statistic to test $H_0: P_1 = P_2$ is $W = \sum_{j=1}^m \text{ranks } R(P_{n_0}, y_j)$. The ranks of $R(P_{n_0}, y_j)$ behave under H_0 as m numbers randomly chosen from $\{1, 2, \dots, n + m\}$. Hence, the distribution of W is the distribution of $\rho_1 + \dots + \rho_m$, where ρ_1, \dots, ρ_m is a sample without replacement of $\{1, 2, \dots, n + m\}$ (see Liu and Singh, 1993). The null hypothesis is rejected when W is small, because this indicates that $R(P_{n_0}, y_j)$ take on average lower values than $R(P_{n_0}, x_i)$, implying that the observations y_j are less deep with respect to P_{n_0} than x_i . The alternative hypothesis is that on average more than 50% of population P_1 is inner or more central than any observation from P_2 , showing that the distributions are not the same.

We have applied this test to real data representing the relative diameter versus the relative height of two groups of trees (Laricio and Radiata). Because of technical restrictions in the measurements, the relative diameter is defined as the ratio between its value at the corresponding height and the diameter at a fixed height (1.3 cm). Relative height is height over the total height of the tree. Figure 11 shows the curves corresponding to 70 Laricio trees (left panel) and 140 Radiata trees (right panel). Because the number of observations per tree is very irregular (from 3–25), the data have been smoothed using a B-spline basis of order three with knots in the argument

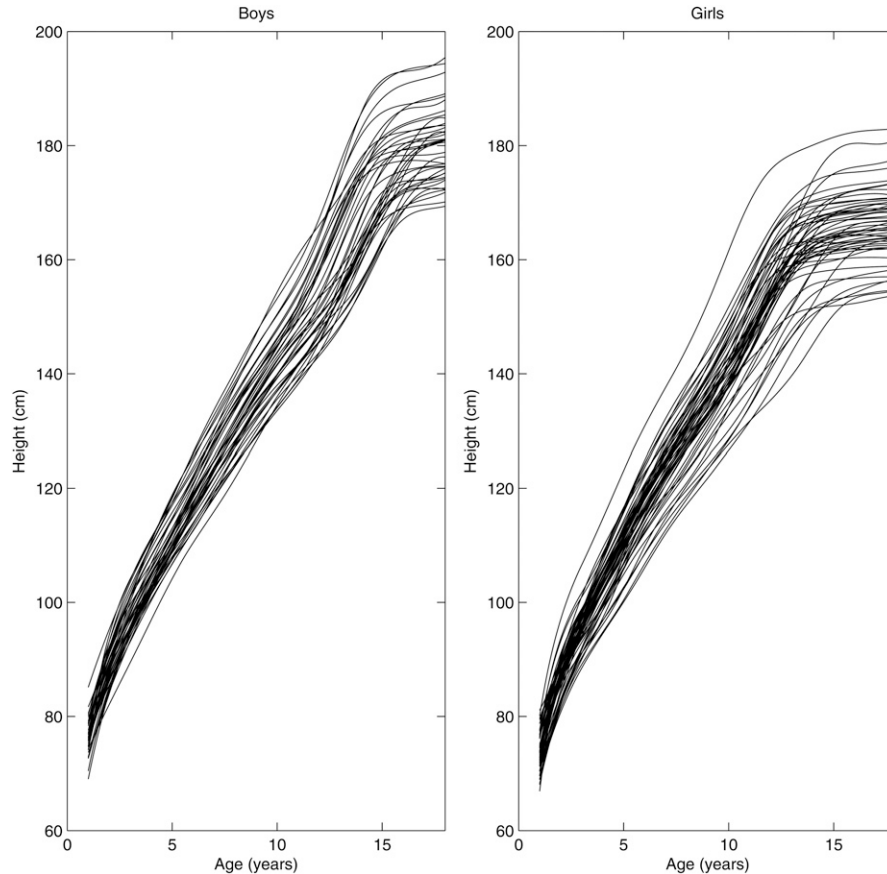


Figure 12. Growth curves for a sample of 30 boys (left panel) and 54 girls (right panel).

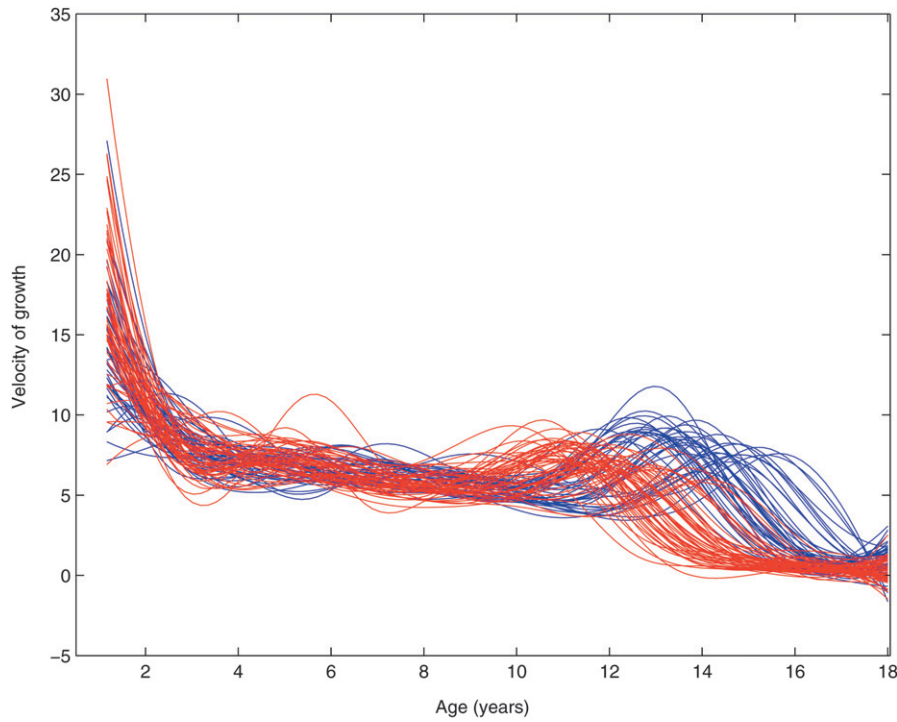


Figure 13. First derivative of the growth curves for boys (in blue) and girls (in red).

values of each curve. To apply the rank test, we have considered 70 functions randomly chosen from the Radiata trees group as the reference group to compute the ranks of the remaining curves. The p -values (defined as the probability of W being smaller than the observed statistic W_{obs}) obtained using all the notions of depth (BD , MBD , FM , and L_1D) are very close to zero. Therefore, we conclude that there exist significant differences between both groups.

The second real dataset includes the growth curves for boys and girls (see Ramsay and Silverman, 2005). We have applied the rank test to decide if there are no differences between both groups curves. We consider 32 curves randomly chosen from the group of girls as the reference group. The remaining 22 curves constitute the test group together with the 30 growth curves for boys. The p -value with BD is 0.0001; hence, we reject the null hypothesis, concluding that there exist significant differences between the growth curves for boys and girls. This difference could be caused by a change either in mean or in dispersion. Graphically, the groups do not seem to be similar (see Fig. 12). The shape is different and the heights of boys achieve higher values at the end. The rank test detects these differences. However, if we apply the rank test using the modified band depth (MBD), Fraiman and Muniz's depth (FM) or Vardi and Zhang's depth (L_1D) instead of BD , we obtain p -values of 0.1199, 0.1636, and 0.001, respectively, concluding in this case that there is no evidence for rejecting the null hypothesis using MBD or FM . The reason is that MBD and FM consider only the magnitudes, ignoring the curves shape. Note that the average values of boys and girls heights only differ in the final years (17–18 years), and FM and MBD do not detect differences between both groups because they occur over a short interval. Because the essential difference between both groups is

shape, we have applied the rank test to the curves derivatives (growth speed) (see Fig. 13). The rank test p -values using BD , L_1D , MBD , and FM are very close to zero ($1.3 * 10^{-4}$, $1.6 * 10^{-4}$, $4.54 * 10^{-7}$, and $6.01 * 10^{-7}$, respectively) and the null hypothesis is rejected. The instant of maximum growth velocity is different for boys and girls (see Fig. 13). Girls reach maximum speed at an earlier age than boys. The band depth rank test detects these shape differences for boys and girls both in the original sample of growth curves and in the derivatives set.

9. CONCLUSIONS

We have introduced new notions of depth for functional data based on the graphic representation of the curves. They provide a simple criterion for ordering a sample of functions from center-outward. Robust statistics for functional observations, such as the median and trimmed mean, can be constructed. The finite-dimensional version of the new band depths are very useful for dealing with high-dimensional data because they are computationally feasible, avoiding the main drawback of other finite-dimensional depth definitions. These new notions satisfy usual depth properties except affine invariance, which is not natural for functional data. We have also established the uniform consistency of the sample band depth in the finite and functional case. Robustness of these new depths is illustrated with a simulation study and several real examples. As an application, a rank test for functional data is introduced and applied to the problem of deciding whether two groups of curves come from the same population.

REFERENCES

- Arcones, M. A., and Giné, E. (1993), "Limit Theorems for U-Processes," *Annals of Probability*, 21, 1494–1542.
- Brown, B. and Hettmansperger, T. (1989), "The Affine Invariant Bivariate Version of the Sign Test," *Journal of the Royal Statistical Society, Ser. B*, 51, 117–125.
- Chaudhuri, P. (1996), "On a Geometric Notion of Quantiles for Multivariate Data," *Journal of the American Statistical Association*, 91, 862–872.
- Cuevas, A., Febrero, M., and Fraiman, R. (2007), "Robust Estimation and Classification for Functional Data via Projection-Based Depth Notions," *Computational Statistics*, 22, 481–496.
- Dyckerhoff, R. (2004), "Data Depths Satisfying the Projection Property," *Allgemeines Statistisches Archiv*, 88, 163–190.
- Fraiman, R., and Meloche, J. (1999), "Multivariate L -Estimation," *Test*, 8, 255–317.
- Fraiman, R., and Muniz, G. (2001), "Trimmed Means for Functional Data," *Test*, 10, 419–440.
- Hettmansperger, T. and Oja, H. (1994), "Affine Invariant Multivariate Multi-sample Sign Tests," *Journal of the Royal Statistical Society, Ser. B*, 56, 235–249.
- Inselberg, A. (1981), " N -Dimensional Graphics, Part I-Lines and Hyperplanes, in IBM LASC," Technical Report, G320-27111.
- Inselberg, A. (1985), "The Plane Parallel Coordinates," Invited paper, *The Visual Computer*, 1, 69–91.
- Inselberg, A., Reif, M., and Chomut, T. (1987), "Convexity Algorithms in Parallel Coordinates," *Journal of the ACM*, 34, 765–801.
- Kemperman, J. H. B. (1987), "The Median of a Finite Measure on a Banach Space," in *Statistical Data Analysis Based on L_1 Norm and Related Methods*, ed. Y. Dodge, Amsterdam: North-Holland, pp. 217–230.
- Koshevoy, G., and Mosler, K. (1997), "Zonoid Trimming for Multivariate Distributions," *The Annals of Statistics*, 25, 1998–2017.
- Li, J., and Liu, R. (2004), "New Nonparametric Tests of Multivariate Locations and Scales using Data Depth," *Statistical Science*, 19, 686–696.
- Liu, R. (1990), "On a Notion of Data Depth Based on Random simplices," *The Annals of Statistics*, 18, 405–414.
- (1995), "Control Charts for Multivariate Processes," *Journal of the American Statistical Association*, 90, 1380–1388.
- Liu, R., Parelius, J. M., and Singh, K. (1999), "Multivariate Analysis by Data Depth: Descriptive Statistics, Graphics and Inference," *Annals of Statistics*, 27, 783–858.
- Liu, R., and Singh, K. (1993), "A Quality Index Based on Data Depth and Multivariate Rank Test," *Journal of the American Statistical Association*, 88, 257–260.
- López-Pintado, S., and Romo, J. (2005), "Depth-Based Classification for Functional Data," in *Data Depth: Robust Multivariate Analysis, Computational Geometry and Applications*, American Mathematical Society, DIMACS Series, eds. R. Liu, R. Serfling, and D. L. Souvaine, 72, 103–121.
- Mahalanobis, P. C. (1936), "On the Generalized Distance in Statistics," *Proceedings of National Academy of Science of India*, 12, 49–55.
- Mosler, K. (2002), *Multivariate Dispersion, Central Regions and Depth: The Lift Zonoid Approach*, New York: Springer.
- Oja, H. (1983), "Descriptive Statistics for Multivariate Distributions," *Statistics & Probability Letters*, 1, 327–332.
- Pollard, D. (1984), *Convergence of Stochastic Processes*, New York: Springer Verlag.
- Ramsay, J. O., and Silverman, B. W. (2005), *Functional Data Analysis*, (2nd ed.), New York: Springer Verlag.
- Rousseeuw, P., and Hubert, M. (1999), "Regression Depth" (with discussion), *Journal of the American Statistical Association*, 94, 388–433.
- Serfling, R. J. (2004), "Nonparametric Multivariate Descriptive Measures Based on Spatial Quantiles," *Journal of Statistical Planning and Inference*, 123, 259–278.
- Singh, K. (1991), "A Notion of Majority Depth," unpublished document.
- Tukey, J. (1975), "Mathematics and Picturing Data," *Proceedings of the 1975 International Congress of Mathematician*, 2, 523–531.
- Vardi, Y., and Zhang, C.-H. (2000), "The Multivariate L_1 -Median and Associated Data Depth," *Proceedings of the National Academy of Sciences of the United States of America*, 97, 1423–1426.
- Wegman, E. (1990), "Hyperdimensional Data Analysis Using Parallel Coordinates," *Journal of the American Statistical Association*, 85, 664–675.
- Wood, A. T. A., and Chan, G. (1994), "Simulation of Stationary Gaussian Processes in $C[0, 1]$," *Journal of Computational and Graphical Statistics*, 3, 409–432.
- Yeh, A., and Singh, K. (1997), "Balanced Confidence Sets Based on the Tukey Depth," *Journal of the Royal Statistical Society, Ser. B*, 3, 639–652.
- Zuo, Y. (2003), "Projection Based Depth Functions and Associated Medians," *The Annals of Statistics*, 31, 1460–1490.
- Zuo, Y., and Serfling, R. (2000a), "General Notions of Statistical Depth Function," *The Annals of Statistics*, 28, 461–482.
- (2000b), "Structural Properties and Convergence Results for Contours of Sample Statistical Depth Functions," *The Annals of Statistics*, 28, 483–499.